Nat Hazards (2014) 74:1309–1326
DOI 10.1007/s11069-014-1252-y

ORIGINAL PAPER

Synoptic features and environmental conditions of the tornado outbreak on March 22, 2013 at Brahmanbaria in the east-central region of Bangladesh

Fatima Akter · Hirohiko Ishikawa

Received: 6 November 2013 / Accepted: 18 May 2014 / Published online: 1 June 2014

Abstract This study evaluates the synoptic features and environmental conditions of Brahmanbaria tornado event that caused 36 fatalities, 388 injuries and huge damages of properties on 22 March, 2013. Various factors for initiation of that terrific event are investigated through analysis JRA-55 reanalysis (50 km horizontal resolution) data and Multi-functional Transport Satellite images by Japan Meteorological Agency. In addition, radar images, radiosonde data and three hourly synoptic data of Bangladesh Meteorological Department are used to verify the reanalysis data. The genesis of the tornadic storm is identifiable in the most unstable part of the study region. The satellite observations are found to useful to identify the location of convection occurrence region. The half hourly satellite images identify that the convection initiation started at the convergence area and the systems intensify and organize by the continuous moisture supply from the Bay of Bengal. Lower-level convergence coupled with strong wind shear and humidity gradient lift moist air aloft to trigger deep convection and the severe storm occurred. Energy Helicity Index seems a good predictor parameter for this specific case study.

Keywords Thunderstorms · Severe local storms · Tornado · Bangladesh disaster · Brahmanbaria tornado · Dryline

1 Introduction

Bangladesh is vulnerable to various natural hazards. Severe local convective storms (hereinafter referred to as SLCS) are one of the most devastating phenomena in the pre-

Present Address:
F. Akter (✉) · H. Ishikawa
Disaster Prevention Research Institute, Kyoto University, Gokasho, Uji, Kyoto 611-0011, Japan
e-mail: fatima_a@storm.dpri.kyoto-u.ac.jp

H. Ishikawa
e-mail: ishikawa@storm.dpri.kyoto-u.ac.jp

monsoon months (March–May) in Bangladesh and adjoining northeastern India. The SLCS accompany gusty wind, heavy downpours and hails after a long dry season, and often spawn tornadoes. SLCS cause huge damages to our lives and properties in a very short period. These storms are locally termed as Nor'wester (*Kalbaishakhi*—in Bengali) since the system migrates from northwest to southeast. Every year the SLCS of Bangladesh cause the highest death toll in the World. Annual death toll accounts for 179 deaths per year caused only from tornadoes in Bangladesh from the period of 1967–1996 (Ono 2001).

On March 22, 2013, a devastating tornado (approximately 15 min) hit the villages in Sadar upazila (regional subdivision—the second lowest administrative unit) (24°N latitude and 91°E longitude) of Brahmanbaria district in east-central region of Bangladesh (Fig. 1a). It was initiated in the afternoon 1055 UTC (the Bangladesh Local Time is UTC + 6 h) and was extinguished at 1110 UTC according to the eye witness. Thirty-six persons were killed and three hundred eighty-eight persons were injured by this event.[1] The tornado left a trail of destruction stretching as long as 12–15 km length passing over 22 villages and the width was approximately 100–150 m. A GPS tracking of the tornado path was conducted by SAARC Meteorological Research Center (SMRC) after the event occurrence (Fig. 1b). The wind speed was approx. 55 m/s. It was identified as F2 category in the Fujita scale.[2]

In the pre-monsoon season, surface warm moist southerly wind blows from the Bay of Bengal toward Bangladesh, whereas surface warm dry westerly wind blows from Indian territory. Strong horizontal moisture gradient is created between these two air masses of different origin. In the mid- and upper-troposphere, there prevails strong cool dry north-westerly wind, which extends to westerly jet over the north-eastern part of Indian sub-continent. Intense insolation of this season heats the dry ground surface and a low heat develops in the lower troposphere over the Indian high land. In contrast, the seasonal high is observed over the Bay of Bengal. Strong moisture gradient, temperature and pressure difference between dry and moist region, significant vertical wind shear and temperature inversion (2 km AGL) over moist side produce great potential instability, and these weather conditions are favorable for frequent and intense convective activities in Bangladesh and northeast India (Weston 1972; Prasad 2006; Yamane and Hayashi 2006; Yamane et al. 2010b). Previous studies also identified that central region of Bangladesh is the most preferred location of SLCS formation in Bangladesh (Peterson and Mehta 1981; Yamane et al. 2010a). From our 16-year study (1990–2005), total 2,324 SLCS events were identified in Bangladesh territory (Yamane et al. 2010a), which means around 145 SLCS events occurs per year on an average. Some other studies focused on the dynamic and thermodynamic aspects of the initiation of SLCS (Yamane et al. 2010b; Murata et al. 2011; Lohar and Pal 1995), or discussed on propagation and modes of organization of mesoscale convective systems (Dalal et al. 2012), and lower-, mid- and upper-tropospheric features for initiation of nor'westers (Ghosh et al. 2008). Mukhopadhyay et al. (2009) explained the formation mechanism of SLCS with interaction of large-scale and mesoscale environment for specific cases over West Bengal. However, the physical process of storm genesis with trigger mechanisms of SLCS organization are not yet well studied in Bangladesh due to the scarcity of observation data in the study area.

In Bangladesh, sparse surface weather stations, four active radar (not full time) and only one upper air sounding at Dhaka (23.7°N latitude and 90.3°E longitude) limit the understanding of severe weather. In the previous studies, it was difficult to see the detailed

[1] Situation Report, Disaster Management Bureau, Bangladesh.

[2] BMD Newsletter, Vol.3, issue 3, May 2013.

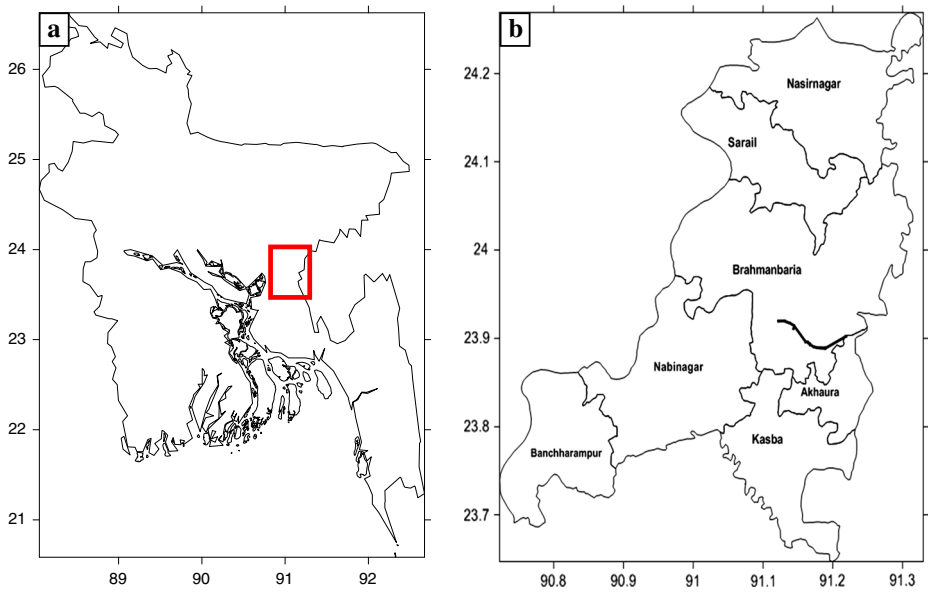

Fig. 1 **a** Bangladesh territory and *red box* indicating Brahmanbaria district; **b** enlarged figure of *red box* indicating track of the tornado. GPS survey was conducted by the researchers of BMD and SMRC after the event occurrence

environmental features for individual events. So, in this paper, we attempt to confirm that reanalysis data successfully analyzes accurate environmental conditions and trigger mechanism of convection initiation for SLCS occurrence in that particular area.

In order to minimize the SLCS disasters, proper prediction of convective event is important. Such a local-scale phenomena as SLCS, however, is very difficult to predict numerically. Instead of predicting SLCS itself, numerical prediction of pre-storm environment is to be used to assess the possibility of SLCS outbreak. In this context, Yamane et al. (2010b, 2012) suggest the use of thermodynamic parameters as guidance to the prediction of possible SLCS, where atmospheric environment has high potential instability on SLCS days of Bangladesh. Though the horizontal resolution was coarse to identify locality of SLCS event in that study, a finer resolution reanalysis data are now available from some meteorological centers. The use of objective analysis will be quite promising in predicting the possibility of SLCS events.

The objective of the paper is to show the role of significant synoptic and environmental features to trigger the formation and intensification of SLCS associated with the tornado that occurred on 22 March, 2013. In this present study, we use 55-year Japanese reanalysis JRA-55 data (0.5625° horizontal resolutions, approximately 50 km) of Japan Meteorological Agency (JMA) to show the detailed environmental condition of the event area.

2 Radar, satellite and synoptic observation on 22 March, 2013

Weather radar images of the tornado event were captured at Cox's Bazar (21.4°N and 92°E) station of Bangladesh Meteorological Department (BMD) (Fig. 2a–d). The image at

0800 UTC shows the emergence of the system (Fig. 2a). The next radar image at 0900 UTC, 2 h before of the event, shows the system was much developed and moved southeastward (Fig. 2b). Then, several convective clouds were developing along a line running from the west–southwest to east–northeast over the Bengal plain. The weather radar image at 1100 UTC, corresponding to the tornado occurrence time, shows that the matured system migrated over the event location (Fig. 2c). The following radar image was 15 min after the event occurrence time that shows relatively weak system crossing the event site (Fig. 2d). The radar was nearly 300 km away from the tornado occurrence site and was out of the Doppler mode observation area. So the detailed structure was not obtained.

IR imageries observed by MTSAT-2 of JMA are also used to see the convective activities. Figure 3a–h shows eight panels of half hourly snaps of IR imageries of MTSAT-2 of 22 March, 2013. The star sign denotes the place of the tornado occurrence. At 0801 UTC[3] (approximately 3 h prior to the event) shows the emergence of small convective cloud (system no. 1) along 90.7°E longitude and 24.3°N latitude (Fig. 3a). This cloud appears to be the genesis of storm. The position of the convective cell is close to the event occurrence site. The cell is seen to have intensified and little extended toward east–southeast direction (Fig. 3b). Figure 3b is overlaid with the 0900 UTC horizontal specific humidity distribution data from BMD, and it shows an area of high specific humidity gradient from southwest to northeast. At 0901 UTC, Fig. 3c shows a signature of new cell (system no. 2) at the southwest of the previous cell. Pioneer cell (system no. 1) is developed a strong convective cell and second one also becomes stronger, and another new signature of convection (system no. 3) is observed at southwest (Fig. 3d). At 1001 UTC (Fig. 3e), three convective cells (systems 1, 2 and 3) are found aligned in a southwest to northeast line and each of which looks like tailing anvil clouds in east–southeast direction. This anvil direction coincides with upper wind direction above 700 hPa. The convective cloud line follows the specific humidity gradient line (referring Fig. 3b again). The pioneer cell (system no. 1) becomes an organized mature system (Fig. 3f).

A tornado occurred at 1055 UTC and continued up to 1110 UTC near 91°E longitude and 24°N latitude. At 1101 UTC, systems 1 and 2 merged together (Fig. 3g), and later, the system 3 joined with the merged system passed through the event area (Fig. 3h). The upper layer cloud (anvil) flows to east–southeast but the system seems to move eastward. The systems are maintained till it dissipated after crossing the event area. The half hourly satellite images suggest the existence of certain triggering mechanism along the heads of a series of convective cells.

3 Data and methodology

SLCS studies are difficult in Bangladesh territory due to its localized characteristics and sparse observation network. Existing observations do not describe the event precisely. So we have to use analysis or reanalysis data. JRA-55 reanalysis data are the world's first atmospheric global reanalysis which covers 55 years (1958–2012) with four-dimensional variational data assimilation system Ebita et al. (2011).[4]

The base model is of TL319L60, so that the horizontal resolution is 0.5625° in longitudinal direction and approximately 0.5625 in latitudinal. It has 60 layers from surface to

[3] The time of MTSAT-2 data refer to the start of full disk scan. The observation time at study area is several minutes after the designated time.

[4] http://jra.kishou.go.jp/JRA-55/index_en.html.

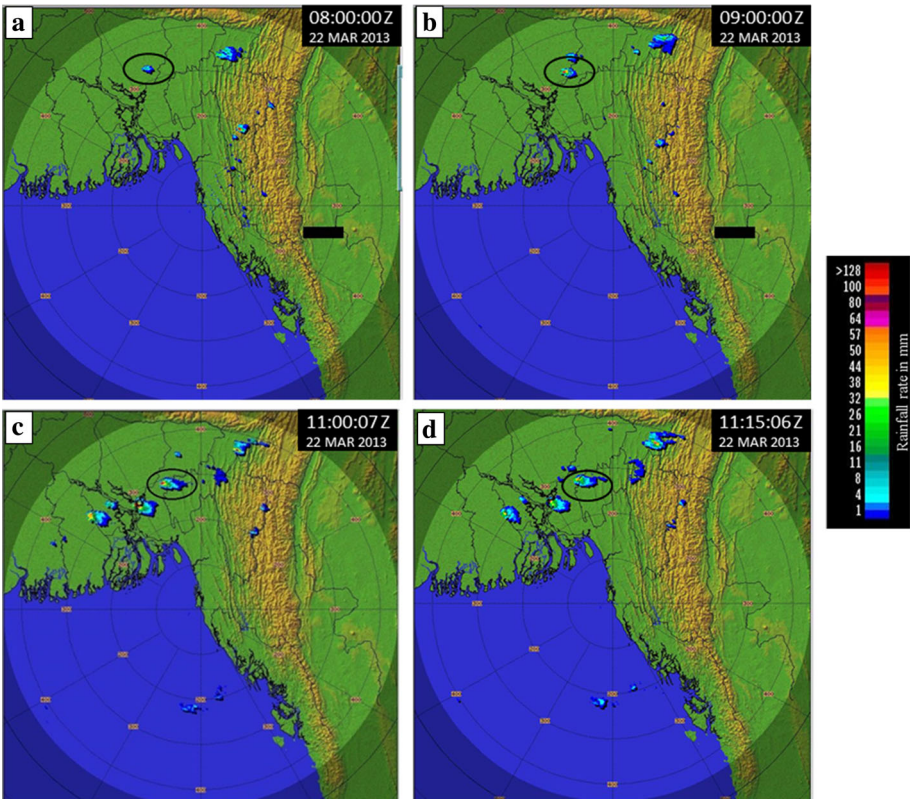

Fig. 2 Cox's Bazar radar images (**a**–**d**). The systems marked with *thick black circle* at **a** 0800 UTC—system emerged, **b** 0900 UTC—system intensified, **c** 1100 UTC—event occurrence time and **d** 1115 UTC—system moved southeast ward. Rainfall intensity is presented in *scale bar*, the *red color* represents rainfall intensity of more than 100 (mm/h). The center of the circle is the radar position, and circles are drawn at every 100 km

0.1 hPa. The vertical resolution is finer near the surface for better representation of the planetary boundary layer processes. The data are provided 6 hourly. Many variables are provided among which we use geopotential heights, wind (zonal and meridional), temperature and specific humidity in this study. These data are supplied in model grid, and we also computed mean sea level pressure (MSLP) and pressure level data at standard levels (1,000, 975, 950, 925, 900, 875, 850, 825, 800, 750, 700, 650, 600, 550, 500, 450, 400, 350, 300, 250, 200, 150, 100, 70 and 50 hPa) for the use in stability parameter calculation.

Before using the reanalysis data, however, it is important to check whether the analysis is in harmony with observed data. We compared JRA-55 reanalysis data to radiosonde data archived at University of Wyoming.[5] Figure 4 shows comparisons of Dhaka radiosonde profile and the profile of reanalysis data at nearest grid to the radiosonde site at the event day. The geopotential height is of course almost identical. The temperature profile is also in good agreement besides slight difference in boundary layer. Horizontal winds show

[5] http://weather.uwyo.edu/cgi-bin/sounding?region=seasia&TYPE=TEXT%3ALIST&YEAR=2013&MONTH=03&FROM=2200&TO=2200&STNM=41923.

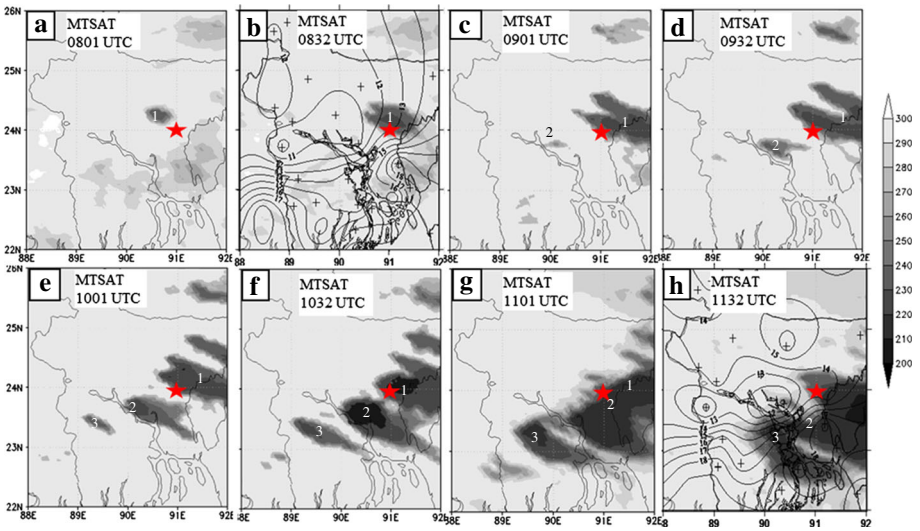

Fig. 3 Shaded 30-min interval black body temperature (TBB) distribution by MTSAT-2 from 0801UTC to 1132UTC on March 22, 2013. Contoured surface-specific humidity (g/kg) distribution of 0900 UTC and 1200 UTC of three hourly BMD SYNOP data overlaid with images (**b**), (**h**), respectively. Systems are recognized by no. *1*, *2* and *3*. "*Star*" sign is event occurring region

some scatter in radiosonde data. The scatter in humidity is rather large in relative humidity. It is not appropriate to say which data are plausible since both data have difference representativeness. A radiosonde data are a snapshot along the path of ascending sensors, whereas the reanalysis represents the average over, at least, grid distance. The statistical performance of JRA-55 reanalysis was also checked with radiosonde observation for March–May in 2013, and the correlation is shown in Table 1. Geopotential height again shows very good correlation in all levels. Temperature also has good correlation almost all levels except for lower levels. Horizontal wind components have good correlation in upper levels, but the correlation decrease in lower levels. Though the correlation is relatively low in some variables in boundary layer, both reanalysis and radiosonde observation are consistent.

To examine environmental stability condition, several stability indices are computed. Convective parameters are K Index (KI), Total Total (TT), Showalter Stability Index (SSI), precipitable water (PW) (kg/m^2), convective available potential energy (CAPE) (J/kg), convective inhibition (CIN) (J/kg) and Lifted Index (LI). Kinematic parameters are mean shear (MS) (m/s), wind shear between the surface and 500 hPa wind (SHEAR0–500 hPa) and storm relative environmental helicity (SREH) (m^2/s^2). Combined parameters relating to the occurrence of tornado are also computed, which are vorticity generation parameter (VGP) (m/s^2), Energy Helicity Index (EHI) and bulk Richardson number (BRN). The physical meaning of the indices is explained in previous works (e.g., Yamane et al. 2010b).

The analysis region is seen in Fig. 5a. Synoptic features are discussed over a domain covering 65°E–100°E and 5°N–29°N (Fig. 5a). The topography of this region contains high land to the western, northern and eastern sides. The Bay of Bengal is situated to the south, and central part is the one of the largest deltas of the world, the Ganges–Brahmaputra–Meghna River delta, that belongs to Bangladesh territory. In the west Chota

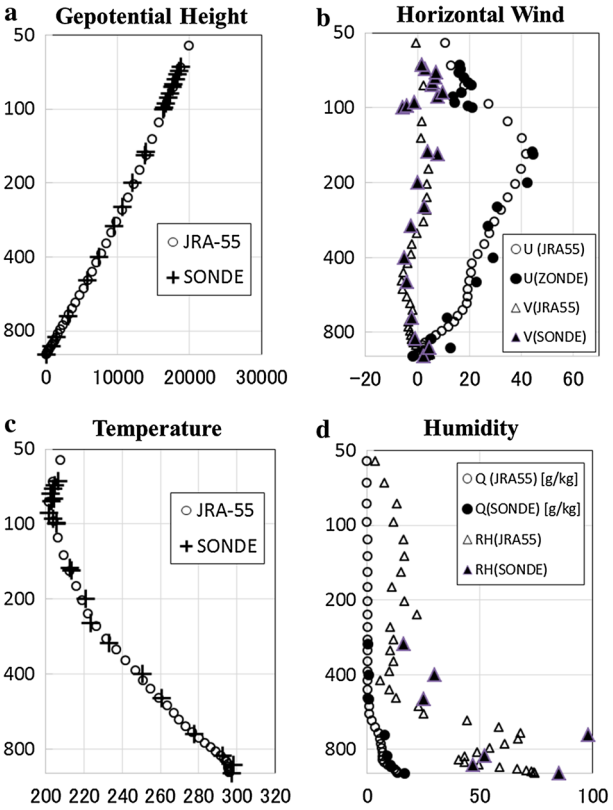

Fig. 4 Vertical profile of radiosonde data and JRA-55 reanalysis model level data of **a** Geopotential Heights, **b** Horizontal Wind (U and V component), **c** temperature, **d** relative humidity (RH) and specific humidity (Q) at 0000 UTC March 22, 2013

Nagpur Plateau (900 m) of India, in the north there are the great Himalayan ranges, in the northeast there are Garo Hills (450 m) and Khashi hills (1,500 m) and in the southeast Chittagong Hill tracts (300 m) and high mountain ranges of Tripura and Mizoram (2,000 m). For the detailed analysis, the analysis domain is taken between 84° and 94°E longitude and 18°–28°N latitude (Fig. 5b). The study area covers almost total land area of Bangladesh. The area belongs to deltaic plain where altitude is <10 m above sea level.

4 Results

4.1 Synoptic features analysis on 22 March, 2013

Atmospheric temperature and wind at the lowest model level, approximately 13 m above model topography, and the MSLP over Indian subcontinent of 22 March, 2013 are shown in Fig. 5a, b. The time is 0600 UTC on March 22, 2013, that is the local noon time and is 5 h prior to the tornado occurrence. High pressure existed over Bay of Bengal. South-westerly wind conveyed warm moist air toward Bangladesh. Westerly wind blows from

Table 1 Data validation table

hPa component	Geopotential heights	Zonal wind(m/s)	Meridional wind(m/s)	Temperature (K)	Specific humidity (g/kg)	Relative humidity (%)
(a) 00 UTC						
1,000	0.983	0.509	0.730	0.546	0.553	0.338
925	0.969	0.750	0.792	0.611	0.699	0.557
850	0.915	0.706	0.692	0.787	0.831	0.716
700	0.899	0.772	0.610	0.936	0.850	0.781
500	0.920	0.890	0.848	0.933	0.810	0.690
300	0.987	0.952	0.853	0.972	0.670	0.597
200	0.993	0.955	0.925	0.939	–	–
(b) 12 UTC						
1,000	0.900	0.630	0.414	0.617	0.593	0.743
925	0.937	0.572	0.761	0.767	0.788	0.722
850	0.916	0.671	0.633	0.771	0.809	0.695
700	0.893	0.755	0.522	0.911	0.823	0.735
500	0.845	0.929	0.851	0.922	0.801	0.736
300	0.971	0.952	0.916	0.970	0.691	0.604
200	0.986	0.970	0.904	0.901	–	–

Pre-monsoon 2013 Correlation Analysis of radiosonde data at Dhaka station and nearest grid point of JRA-55 reanalysis data at (a) 0000 UTC and (b) 1200 UTC

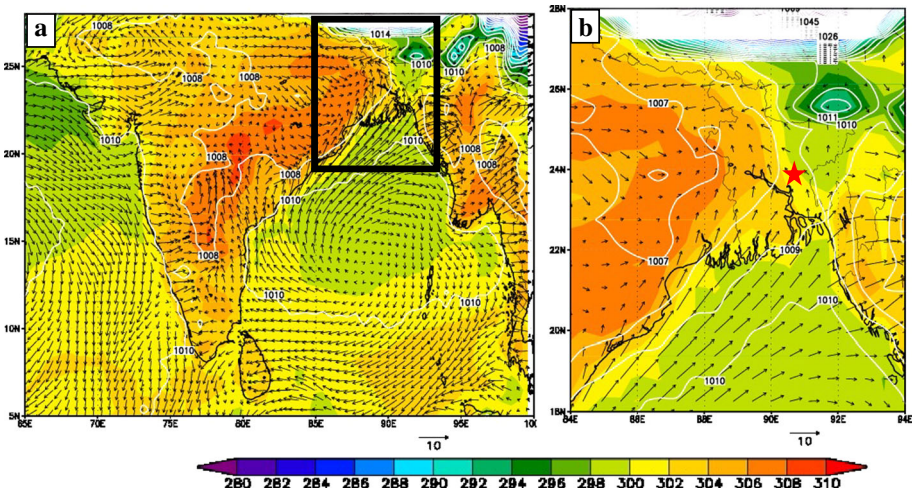

Fig. 5 Surface shaded temperature (K), vector wind (m/s) at lowest model level (approx. 13 m) and contoured MSLP (hPa) distribution at 0600 UTC over **a** Indian Subcontinent, *black box* indicating the smaller domain; **b** Bangladesh region (enlarged figure of *red box*) on March 22, 2013, by JRA-55 reanalysis data

Indian highland toward Bangladesh. Surface air temperature was high in dry Indian highland but was relatively low over Bangladesh territory. The surface temperature increased more than 10° over Indian subcontinent from 0000 UTC (0600 BST) to 1200 UTC (1800 BST), but it was several degrees in Bangladesh. At 0600 UTC, warm advection is analyzed near south coast toward the Bangladesh (fig. not shown). This warm moist advection can bring instability in lower atmosphere. In the morning, easterly wind component was prominent near the surface, Fig. 4b. Wind shear between surface and 500 hPa was 23.2 at 0000 UTC at event location (24°N and 91°E). At 0600 UTC, it slightly increased to 23.3 m/s wind shear between surface southeasterly wind (1.6 m/s) and the 500 hPa westerly wind (20.5 m/s). It further strengthened to 24.3 m/s at 1200 UTC around event site. This wind shear was rather stronger than the statistical value in SLCS days as calculated by Yamane et al. (2010b) and was attributed to the tough upper layer as discussed in Yamane et al. (2012).

Surface-specific humidity was higher over Bangladesh territory than west side of Indian territory. Specific humidity distribution (Fig. 6a–c) exhibited higher values near the coast than the inland. That is consistent with the pre-monsoonal climatological studies by Romatschke et al. (2010) over this region. Surface-specific humidity ranged from 10 to 15 g/kg over Bangladesh. In contrast, the surface-specific humidity was lower, typically between 6 and 10 g/kg over West Bengal of India. It reached to 15 g/kg at 0600 UTC around the east-central region where the event occurred (Fig. 6b). It was evident that southern, eastern and central region became much moist than the north-western region of Bangladesh. Temperature increased slowly over the moist east side than Indian dry area (Fig. 5b). Looking at the vertical cross section at 24°N latitude at 0600 UTC (Figure is not shown) east to west, decrease of specific humidity is analyzed between 84°E and 94°E longitude and vertically from surface to about 600 hPa. The sharp change of specific humidity was specifically seen 88.5°E–90.5°E (10–15 g/kg) in the lower level up to about 900 hPa without any detectable inclination, and west of this specific humidity was decreased 10–6 g/kg.

In relation to storm genesis in Great Plains in the USA, a line of moisture discontinuity, which is termed as dryline, has been discussed. Dryline is a mesoscale narrow boundary that separates moist maritime tropical air masses of Gulf of Mexico from continental tropical dry air masses of the deserts in the western Great Plains in the USA during the warm season (Fujita 1958; Miller 1959; Rhea 1966). During the spring and early summer, the convective storms are frequently initiated along the dryline. Thus, we examine specific humidity gradient in the present case. The strength of specific humidity gradient is computed by

$$|\nabla \cdot q| = \sqrt{\left(\frac{\partial q}{\partial x}\right)^2 + \left(\frac{\partial q}{\partial y}\right)^2},$$

where q is specific humidity (g/kg). In this study, we calculate specific humidity gradient g/kg over 100 km and identify maximum gradient line as dryline from the plot.

Dryline in our case was a line of strong moisture gradient between warm dry air mass of Indian highland and moist air mass of Bay of Bengal, which was aligned in southwest to northeast direction (Fig. 6a–c). This line also coincides with the direction of cloud line (Fig. 3f). From 0600 UTC to 1200 UTC, strong gradient region (6 g/kg/100 km) moved eastward and squeezed, and the sharpest moisture gradient (10 g/kg/100 km) reached to 88.5°E longitude at 1200 UTC (Fig. 6c). Though the analysis time (1200UTC) is 1 h after the event, we can assume that the stronger gradient existed before the event occurrence.

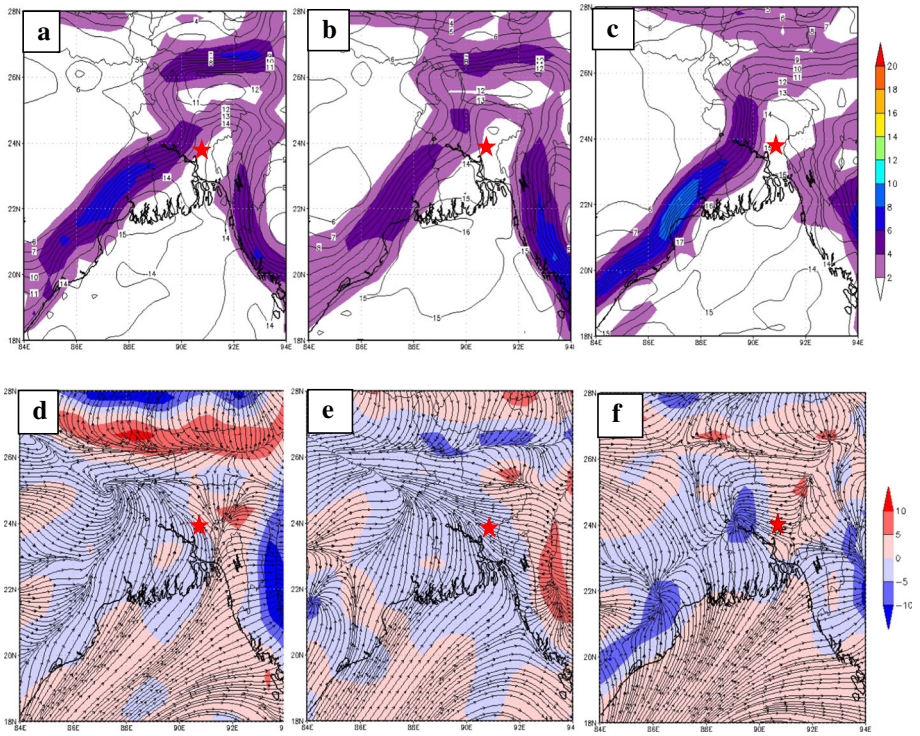

Fig. 6 Shaded surface-specific humidity gradient (g/kg/100 km) and contoured surface-specific humidity (g/kg) distribution at **a** 0000 UTC, **b** 0600 UTC and **c** 1200 UTC; and *shaded surface divergence* and *streamline wind* (m/s) at **d** 0000 UTC, **e** 0600 UTC and **f** 1200 UTC over Bangladesh on March 22, 2013, by JRA-55 reanalysis data

Drylines are known as the zones of enhanced surface convergence in the Great Plains in USA. Strong surface horizontal convergence also coincided with dryline in our study area. Horizontal divergences are shown in Fig. 6d–f. We computed horizontal divergence,

$$\operatorname{div} \boldsymbol{v} = \frac{\partial u}{\partial x} + \frac{\partial v}{\partial y}.$$

Negative divergence is referred to as convergence. The greatest enhancement of low-level convergence was computed in the area where continental westerly flow encounters maritime southwesterly or southerly flow (Fig. 6d–f). This was also the place of the most intense moisture gradient (Fig. 6a–c).

4.2 Atmospheric stability conditions on 22 March, 2013

Atmospheric instability is a major determinant to estimate the possibility of the development of SLCS. Yamane and Hayashi (2006) have evaluated environmental conditions for the formation of severe local storms across the Indian subcontinent and mentioned high thermal instability and vertical wind shear occur in Bangladesh and the northeastern India during the pre-monsoon season.

The Skew-T Log-P is one of the most commonly used thermodynamic diagrams in weather analysis and forecasting using radiosonde soundings. The upper-level sounding is available only at 0000 UTC at Dhaka. We referred to Wyoming Skew-T Log-P analysis of the upper wind sounding at 0000 UTC launched at Dhaka station. High instability is identified where CAPE was 1,690 J/kg at 0000 UTC by Wyoming products (Fig. 7a). CAPE value is analyzed comparatively low value as 1,409 J/kg by JRA-55 reanalysis data at the nearest grid to Dhaka station at 0000 UTC due to different calculation methods using different vertical levels (Fig. 7b). Though the plot suggests favorable atmospheric condition for convective initiation, Dhaka station is about 110 km apart from the event site. Skew-T Log-P diagram is also plotted with JRA-55 reanalysis data at the nearest grid point to event location (91°E longitude and 24°N latitude) on 22 March in Fig. 7c–e together with wind profile. Plot shows CAPE 1,381 J/kg at 0000 UTC. Easterly wind was prominent at surface, and wind veers upward. Strong westerly wind was analyzed at 300 hPa (Fig. 7c). At 0600 UTC about 5 h prior to the event occurrence analysis, an inversion of temperature was evident from 950 to 900 hPa (Fig. 7d). Southeasterly to southerly wind became prominent and surface convergence influenced upward motion. Low-level clockwise wind veer and strong westerly wind increase around 450 hPa are also analyzed. It also shows high CAPE (2,207 J/kg) value. Instability decreased (CAPE 1,282 J/kg) at 1200 UTC after the event occurrence (Fig. 7e).

In Table 2, the values of various stability parameters of present case are compared with statistical values. The last three columns present the values computed from JRA-55 data at the nearest grid of event site for 0000, 0600 and 1200 UTC. In the first two columns, the statistical values of these parameters obtained for SLCS days (Yamane et al. 2010b) are shown. Mean and median values for all indices of SLCS days and non-SLCS days were determined with statistical significance with the confidence level of 99 % (except for the TTI). Since their values are calculated with Dhaka rawinsonde data, the parameters are also computed from Dhaka radiosonde data and JRA-55 values near Dhaka at 0000 UTC, which also listed in the third and fourth column.

It should be noted that there are differences in vertical resolution of different data sources. Yamane et al. (2010b) used very raw rawinsonde observation of data, whereas JRA-55 data have 30 levels between surface and 200 hPa as seen in Fig. 4. Further, our Dhaka radiosonde values in the third column are computed from standard level data only. This difference may affect the values of CAPE, CIN, MS, SREH and the combined parameters slightly, but others are not since they are computed from standard level data.

The comparison between statistical mean values and current values in Table 2 suggested that the environment was unstable from the early morning. Most of the convective parameters were in unstable regimes and met the favorable condition for SLCS occurrence at 0000 UTC and 0600 UTC except for PW. At 0000 UTC, CAPE value already exceeded the statistical mean value, and the energy continued to accumulate till 0600 UTC. At 1200 UTC, 1 h after the event occurrence, the CAPE value decreased in reanalysis data. It seems that a storm may have occurred in the reanalysis modeling. SSI value was favorable only at 0000 UTC. For kinematic parameters only, SHEAR0–500 hPa shows increased shear as day advances and favorable for convection initiation comparing to mean values. Among the combined parameters, EHI indicates >1 at 0600 UTC, which suggests preferable condition for supercell storm occurrences. These favorable conditions have reduced at 1200 UTC, one hour after the event occurrence. Dhaka radiosonde and JRA-55 reanalysis data have difference in CAPE, CIN, SREH and combined parameters. JRA-55 analyzed little lower values than radiosonde data. Dhaka radiosonde data also showed very favorable condition at 0000 UTC though the event site is 110 km apart from the radiosonde site.

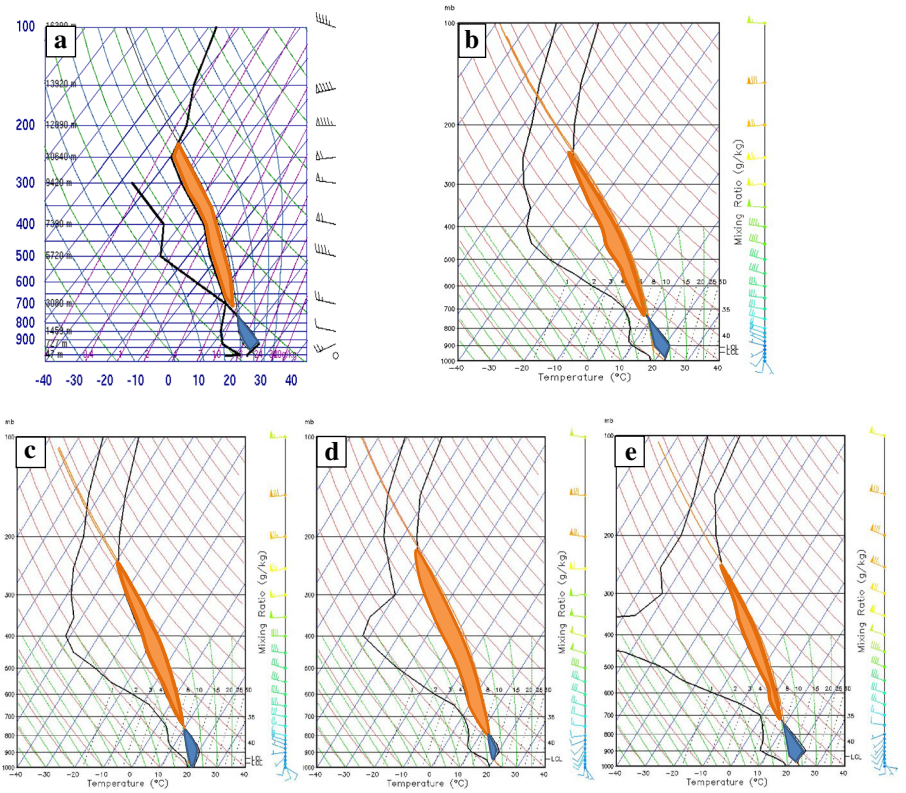

Fig. 7 Skew-T Log-P analysis at 0000 UTC of **a** Dhaka station radiosonde data from University of Wyoming archive, **b** JRA-55 reanalysis data at nearest grid of Dhaka Station; Skew-T Log-P by JRA-55 reanalysis data of event location (24°N latitude and 91°E longitude) at **c** 0000 UTC, **d** 0600 UTC and **e** 1200 UTC on March 22, 2013

We also referred to the proposed threshold values for respective parameters of SLCS occurrence by various authors (Fuelbarg and Biggar 1994; Sadowski and Rieck 1977; Showalter 1953; Galway 1956; Huschke 1959; Moncrieff and Miller 1976; Colby 1984; Rasmussen and Blanchard 1998; Rasmussen and Wilhemson 1983; Davies and Johns 1993; Hart and Korotky 1991; Davies 1993; Weisman and Klemp 1982) and confirmed that the current values suggest the environment truly unstable before the storm genesis.

In order to judge which stability indices are able to predict of the pre-storm environment and possibility of SLCS occurrence, we investigated spatial distribution of those parameters. Spatial distribution of CAPE (J/kg) is shown over Bangladesh (Fig. 8a–c). CAPE values were high in the moist region, and it significantly increased as the day advances. At 0000 UTC, the environment exhibited little instability (Fig. 8a). Later at 0600 UTC, the environment revealed more favorable for storm genesis (Fig. 8b). CAPE reached more than 2,000 (J/kg) over the moist area before the event. At 1200 UTC, CAPE is decreased (Fig. 8c). One day temporal analysis of CAPE at the cross section of 24°N latitude (Fig. 8d) revealed that the event area was most unstable before the convection initiation.

Spatial distribution are also analyzed for SHEAR0–500 hPa, SREH, EHI, LI, PW, KI, SSI, TTI and CIN at 0600 UTC of the event day. Unstable value of SHER 0–500 $>$ 23,

Table 2 Comparison table

Parameters	DHK00Z SLCS days Mean	DHK00Z SLCS days Median	DHK00Z Sonde data	DHK00Z JRA-55 data	BB00Z JRA-55 data	BB06Z JRA-55 data	BB12Z JRA-55 data
Convective							
KI (K)	27.6	29	**41.2**	**32.7**	**31.3**	**31.3**	**31.7**
TT (K)	68	66.9	**70.2**	**72.5**	**74.2**	**70.5**	**81.5**
SSI (K)	0.8	0.7	**−3.5**	**−0.4**	**−0.9**	1.7	1.1
LI (K)	−0.2	0.1	**−3.8**	**−2.7**	**−3.17**	**−2.70**	**−0.84**
PW (kg/m^2)	38.2	38.5	**49.5**	31.0	32.4	33.6	29.3
CAPE (J/kg)	1,363	1,170	**1,690**	**1,409**	**1,381**	**2,207**	**1,282**
CIN (J/kg)	322	300	**278**	192	147	36	192
Kinematic							
SHEAR0–500 hPa (m/s)	16.7	16.5	**23.7**	**23.6**	**23.2**	**23.3**	**24.3**
MS0–1 km (m/s)	20	19.2	**27.7**	11.6	13.7	7.7	7.9
MS0–2 km (m/s)	16.7	16.2	13.9	9.8	10.4	7.2	5.7
MS0–3 km(m/s)	15	14.6	11.3	8.2	8.7	6.2	5.2
MS0–4 km(m/s)	14.3	13.9	8.5	7.6	7.7	6.4	5.7
SREH (m^2/s^2)	148	115	115	39	75	75	60
Combined							
VGP0–1 km (m/s^2)	0.59	0.58	1.20	0.41	0.51	0.36	0.28
VGP0–2 km (m/s^2)	0.51	0.46	0.60	0.35	0.39	0.34	0.21
VGP0–3 km (m/s^2)	0.46	0.42	0.49	0.29	0.32	0.29	0.19
VGP0–4 km (m/s^2)	0.44	0.42	0.37	0.27	0.29	0.30	0.21
EHI	1.32	0.43	**1.36**	0.31	0.65	1.05	0.49
BRN	16.1	7.4	**20.53**	6.63	7.9	9.14	4.70

Statistical mean (column 1) and median value (column 2) of convective parameters at 0000 UTC in Dhaka on SLCS days of Yamane et al. (2010b) are compared with Dhaka 0000 UTC sonde data (column 3) and Dhaka 0000 UTC with JRA-55 reanalysis data (column 4), Brahmanbaria at 0000 UTC, 0600 UTC and 1200 UTC JRA-55 reanalysis data on event day

The bold text represents that the value is in preferable site for storm genesis referencing to former studies

DHK = Dhaka Station

BB = Brahmanbaria (event location)

KI > 30 and TTI > 70 cover large area around event site at 06 UTC, so that these parameters are difficult to identify the event location. EHI greater than one was identified in very narrow zone pointing to the area of potential supercell storm occurrences (Fig. 9a). EHI is used to identify tornado potential by combining total CAPE with SRH in the lower 3 km. CAPE is identified relatively larger area in the moist side of dryline. The SRH which is calculated storm motion using mean wind speed from 0 to 6 km, is a measure of potential for cyclonic updraft produced through the tilting of horizontal vorticity by storm relative inflow. SRH (<100 m^2/s^2) in our study region did not reach the mean value (148 m^2/s^2) of Yamane et al. (2010b) 5 h prior to the event but high SRH extended over the area of high CAPE. Thus due to the increased wind speed within a convectively unstable area EHI indicates much specified area for severe outbreak. LI is analyzed less than −2 (Fig. 9c), and low value of SSI is analyzed (Fig. 9e) around event occurrence

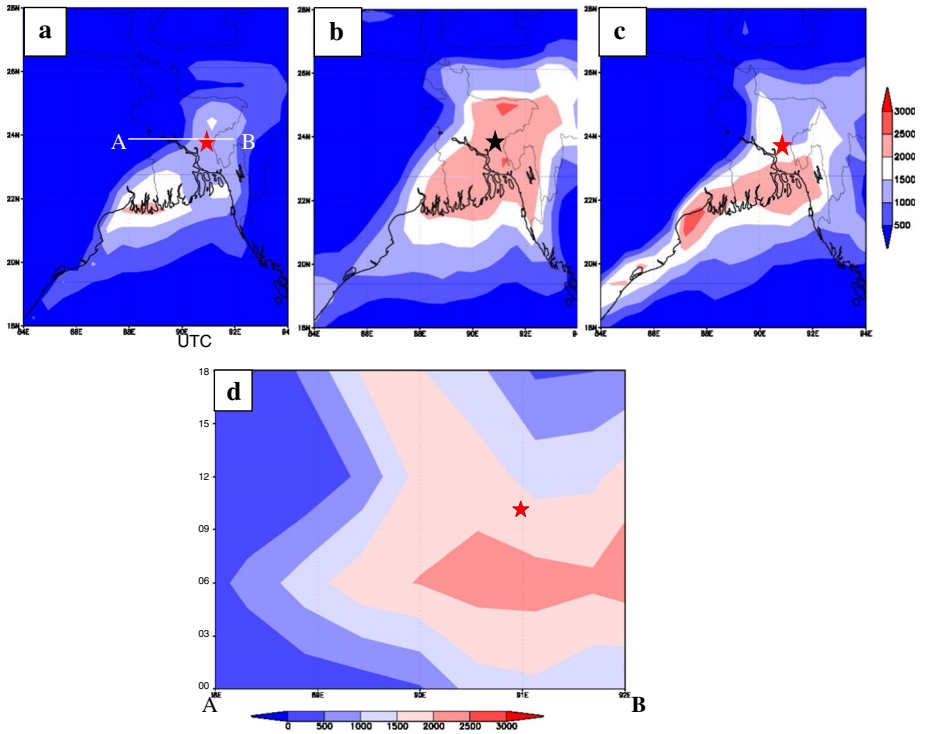

Fig. 8 Shaded CAPE (J/kg) distribution over Bangladesh at **a** 0000 UTC and **b** 0600 UTC, **c** 1200 UTC and **d** time series at the cross section of 24°N latitude (*A–B line* as **a**) from 0000 UTC to 1800 UTC on March 22, 2013, by JRA-55 reanalysis data

regions better than other indices. At 0600 UTC, environment was unstable but convection started 2 h later at 0800 UTC from satellite images (Fig. 3a). The critical condition formed between the two analysis times. One day temporal analysis at the cross section of 24°N latitude of EHI (Fig. 9b) and LI (Fig. 9d) also revealed that the event area was most unstable before the event occurring time. Negative LI exists over relatively wide area and continuing long time after the event occurrence and most negative value of SSI exists after the event at 1200 UTC at the northwest of the event site (Fig. 9f). Among all of these indices, EHI was a good prediction parameter of this event.

5 Discussions

Convection initiation along dryline depends on the synoptic and localized environment features of dryline where surface convergence is enhanced which promotes upward motion consequently air parcelforce to their LFC in an unstable environment to initiate convection. The processes of localized deep convection and developments along the drylines were well investigated in the Great Plains (Bluestein and Parker 1993; Ziegler and Rasmussen 1998; Hane et al. 1997).

Synoptic features and environmental conditions vary distinctly between dry side and moist side of the dryline. At the dry side, temperature increased and thermal low developed

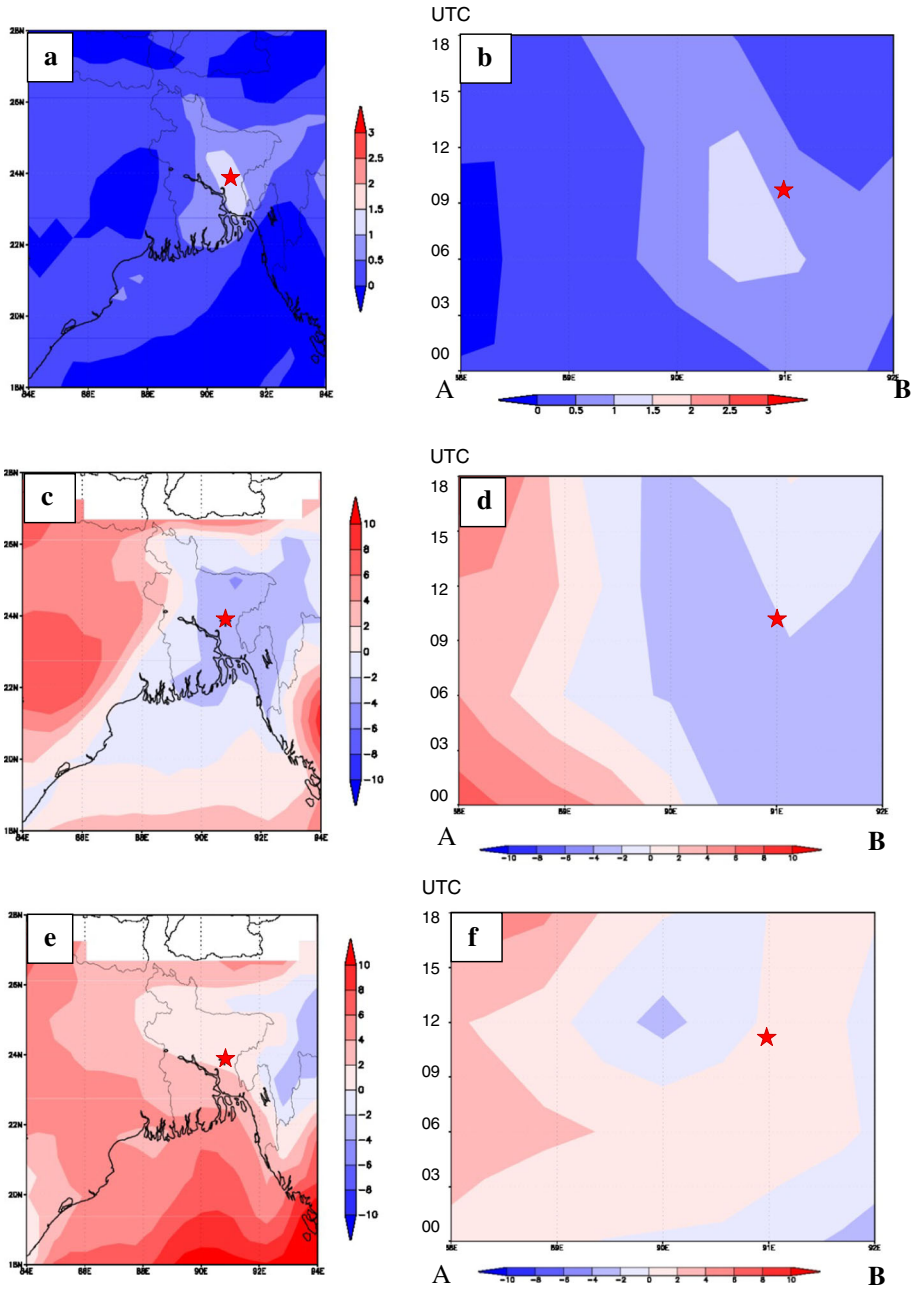

Fig. 9 Spatial distribution of **a** EHI, **c** LI, and **e** SSI at 0600 UTC and time series **b** EHI, **d** LI and **f** SSI at the cross section of 24°N latitude (*A–B line* as Fig. 8**a**) from 0000 UTC to 1800 UTC on March 22, 2013, by JRA-55 reanalysis data

in Indian highland as the day advances (Fig. 5b). Diurnal difference of surface temperature was 10° or more over Indian subcontinent from morning to evening. A deep, well-mixed dry layer developed over the Indian highland from ground to about 680 hPa (Figure not includes). Westerly wind was analyzed in all levels and no wind veer in low level. Strong Jet prevailed over this region above 300 hPa. This deep upper westerly wind advected the deep mixed layer eastward side, and it overlaid on surface moist southwesterly to southerly moist tongue.

As the day advances, increase of surface temperature was smaller at moist side than dry side by few degrees. High MSLP was analyzed over Bay of Bengal and east side of dryline over Bangladesh territory. Surface winds turn toward the dryline and results in enhanced surface convergence at the dryline, which can enhance lift and aid convective initiation. In the current case, surface convergence induced upward motion near dryline. As day advances, CAPE increased due to enhanced moisture incursions in the lower level from the Bay of Bengal at the east side of the dryline. But elevated mixed layer above the moist region acted like cap or lid over the moist region and protected release of instability. Dryline advanced to the east and moisture gradient squeezed and localized convergence became stronger and lifted moist air aloft. Eventually, it forced air parcels to break the lid and reach their LFC to trigger deep convection. Presence of westerly wind and strong wind shear maintained and enhanced the triggered convection and the westerly wind also conveys this system to eastward. The system intensified and became matured enough to spawn as tornado at Brahmanbaria. This mechanism is very similar to the Great Plains convection intimation along dryline as mentioned in Hane et al. 1997, Murphey et al. 2006 and Ziegler and Rasmussen 1998.

There can be another question how much the event day differ from other days. In order to check the uniqueness of the event day, we also analyzed two days (March 20 and 21, 2013) before the event day. Pre-monsoon weather condition was prevailing similar to event day. But, specific humidity (8–12 gm/kg at 0600 UTC) and SHEAR0–500 hPa (12–14 m/s) were relatively low over Bangladesh territory. As day advanced to 1200 UTC, moisture intrusion is analyzed with a little increase of SHEAR0–500 hPa in coastal area. For these two non-event days, surface temperature increase was more rapid from morning to evening and the low-level humidity was less than the event day over Bangladesh. Convergence along dryline was not strong enough due to weak moisture inflow. Surface low moisture cannot create enough instability. Thus, weak convergence along dryline could not uplift air parcel to LFC on non-event days.

6 Summary

In the present study, we examined the synoptic features and environmental conditions for the tornado case on 22 March, 2013, that is the severest in the recent past occurrences. SLCS studies are very difficult in the study region due to its localized characteristics and sparse observation network. Convective parameters and synoptic conditions for the particular case are computed by 50-km-resolution JRA-55 reanalysis data. This case study suggests that low-level convergence along dryline lift the lower atmosphere up to the level of free convection in a significantly unstable environment, where the initial convection triggered. Environmental condition is very favorable for severe convection and storm initiation comparing it with statistical data. EHI is a good predictor to identify SLCS occurrence place. In the previous studies, the data resolution was poor, so that the regional preference of storm genesis is not known. The use of good-resolution reliable and

homogenous data may produce better prediction of severe storm in this area. It is also suggested that better time resolution data is required for pointing the high-risk regions.

Acknowledgments The JRA-55 reanalysis data of JMA used in this study was provided by way of Meteorological Research consortium, a framework for research cooperation of JMA and Meteorological Society of Japan (MSJ). I am grateful to Prof. Hayashi T, Dr. Yamane Y and Dr. Murata F for their valuable suggestions and discussions. I am also thankful to Mr. Abdul Mannan for providing 3 hourly Synoptic data and Radar data from BMD.

References

Bluestein HB, Parker SS (1993) Modes of isolated, severe convective storm formation along the dryline. Mon Weather Rev 121:1354–1372

Colby FP (1984) Convective inhibition as a predictor of convection during AVE-SESAM-2. Mon Weather Rev 112:2239–2252

Dalal S, Lohar D, Sarkar S, Sadhukhan I, Debnath GC (2012) Organizational modes of squall-type mesoscale convective systems during premonsoon season over eastern India. Atmos Res 106:120–138

Davies JM (1993) Hourly helicity, instability, and EHI in forecasting supercell tornadoes. In: Proceedings of 17th conference on severe local storms. St. Louis, MO, American Meteorological Society, pp 107–111

Davies JM, Johns RH (1993) Some wind and instability parameters associated with strong and violent tornadoes. 1. Wind shear and helicity, In: Curch C, Burges D, Doswell C, Davies-Jones R (eds) The Tornado: its structure, dynamics, prediction, and hazard. Geophys Monogr No. 79, Am Geophys Union, pp 573–582

Ebita A, Kobayashi S, Ota Y, Moriya M, Kumabe R, Onogi K, Harada Y, Yasui S, Miyaoka K, Takahashi K, Kamahori H, Kobayashi C, Endo H, Soma M, Oikawa Y, Ishimizu T (2011) The Japanese 55-year reanalysis "JRA-55": an interim report. SOLA 7:149–152

Fuelbarg HE, Biggar DG (1994) The preconvective environment of summer thunderstorms over the Florida Panhandle. Weather Forecast 9:316–326

Fujita TT (1958) Structure and movement of a dry front. Bull Am Meteorol Soc 39:574–582

Galway JG (1956) The lifted index as a predictor of latent instability. Bull Am Meteorol Soc 37:528–529

Ghosh A, Lohar D, Das J (2008) Initiation of Nor'wester in relation to mid-upper and low-level water vapor patterns on METEOSAT-5 images. Atmos Res 87:116–135

Hane CE, Bluestein HB, Crawford TM, Baldwin ME, Rabin RM (1997) Severe thunderstorm development in relation to along-dryline variability: a case study. Mon Weather Rev 125(2):231–251

Hart JA, Korotky W (1991) The SHARP workstation v1.50 users guide. National Weather Service, NOAA, US. Department of Commerce, p 30

Huschke RE (1959) Glossary of meteorology. American Meteorological Society, Boston 638

Lohar D, Pal B (1995) The effect of irrigation on pre-monsoon season precipitation over south West Bengal, India. J Clim 8(1995):2567–2570

Miller RC (1959) Tornado-producing synoptic patterns. Bull Am Meteorol Soc 40:465–472

Moncrieff M, Miller MJ (1976) The dynamics and simulation of tropical cumulonimbus and squall lines. Q J R Meteorol Soc 102:373–394

Mukhopadhyay P, Mahakur M, Singh HAK (2009) The interaction of large scale and mesoscale environment leading to formation of intense thunderstorms over Kolkata Part I: Doppler radar and satellite observations. J Earth Syst Sci 118(5):441–466

Murata F, Terao T, Kiguchi M, Fukushima A, Takahashi K, Hayashi T, Arjumand H, Bhuiyan MSH, Choudhury SA (2011) Daytime thermodynamic and airflow structures over northeast Bangladesh during the pre-monsoon season: a case study on 25 April 2010. J Meteorol Soc Jpn 89A:167–179

Murphey HV, Wakimoto RM, Flamant C, Kingsmill DE (2006) Dryline on 19 June 2002 during IHOP, part I: airborne Doppler and LEANDRE II analyses of the thin line structure and convection initiation. Mon Weather Rev 134:406–430

Ono Y (2001) Design and adoption of household tornado shelters to mitigate the tornado hazard in Bangladesh. PhD Dissertation, Kent State University

Peterson RE, Mehta KC (1981) Climatology of tornadoes of India and Bangladesh. Arch Meteorol Geophys Bioklimatol Ser B 29:345–356

Prasad K (2006) Environmental and synoptic conditions associated with no'westers and tornadoes in Bangladesh—an appraisal based on numerical weather prediction (NWP) guidance products. 14th report of SAARC Meteorological Research Center, Dhaka, Bangladesh

Rasmussen EN, Blanchard DO (1998) A baseline climatology of sounding derived supercell and tornado forecast parameters. Weather Forecast 13:1148–1164

Rasmussen EN, Wilhemson RB (1983) Relationships between stormcharacteristics and 1200 GMT hodographs, low-level shear, and stability. In: Proceedings of 13th conference on severe local storms, Tulsa, OK: American Meteorological Society, pp J5–J8

Rhea JO (1966) A study of thunderstorm formation along dry lines. J Appl Meteorol 5:58–63

Romatschke U, Medina S, Houze RA (2010) Regional, seasonal, and diurnal variations of extreme convection in the south Asian region. J Clim 23:419–439

Sadowski AF, Rieck RE (1977) Technical procedures bulletin no. 207: stability indices. National Weather Service, Silver Spring, p 8

Showalter AK (1953) A stability index for thunderstorm forecasting. Bull Am Meteorol Soc 34:250–252

Weisman ML, Klemp JB (1982) The dependence of numerically simulated convective storms on vertical wind shear and buoyancy. Mon Weather Rev 110:504–520

Weston KJ (1972) The dry-line of northern India and its role in cumulonimbus convection. Q J R Meteorol Soc 98(417):519–531

Yamane Y, Hayashi T (2006) Evaluation of environmental conditions for the formation of severe local storms across the Indian subcontinent. Geophys Res Lett 33:L17806

Yamane Y, Hayashi T, Dewan AM, Akter F (2010a) Severe local convective storms in Bangladesh: part 1. Climatol Atmos Res 95:400–406

Yamane Y, Hayashi T, Dewan AM, Akter F (2010b) Severe local convective storms in Bangladesh: part 2. Environmental conditions. Atmos Res 95:407–418

Yamane Y, Hayashi T, Kiguchi M, Akter F, Dewan AM (2012) Synoptic situations of severe local convective storms during the pre-monsoon season in Bangladesh. Int J Climatol 33:725–734

Ziegler CL, Rasmussen EN (1998) The initiation of moist convection at the dryline: forecasting issues from a case study perspective. Weather Forecast 13:1106–1131